World Journal of Advanced Engineering Technology and Sciences
eISSN: 2582-8266
Cross Ref DOI: 10.30574/wjaets
Journal homepage: https://wjaets.com/

(RESEARCH ARTICLE)

Check for updates

Slurry erosion wear of high chromium cast iron samples from a slurry pump impeller. Effect of impact angle variation

Chaves Pereira da Silva, Renato [1], Barbosa, Paulo Ricardo [1], Penagos, José Jimmy [2] and Rodrigues da Costa Adilson [1,*]

[1] *Federal University of Ouro Preto - Ouro Preto School of Mines, REDEMAT - Thematic Network in Materials Engineering - Praça Tiradentes, 20 - CEP: 35400-000, Ouro Preto, MG – Brazil.*
[2] *Vale Technological Institute – Mining – UFOP Campus - CEP: 35400-000, Ouro Preto, MG – Brazil.*

World Journal of Advanced Engineering Technology and Sciences, 2023, 08(02), 275–286

Publication history: Received on 04 April 2023; revised on 05 April 2023; accepted on 08 April 2023

Article DOI: https://doi.org/10.30574/wjaets.2023.8.2.0106

Abstract

In this work, the impact angle effect on the erosive wear resistance of high chromium cast iron (HCCI) samples from a slurry pump impeller was evaluated. For this purpose, equipment was designed and built to carry out wet erosion tests. Erosion tests were carried out at angles of 30°, 45°, 60° and 90° using an erosive slurry with a concentration of 20%, by weight, of silica sand. The results indicated that the erosive wear rate followed the classic behavior of variation with the impact angle for ductile materials. There was an increase in the erosion rate with increasing angle until reaching the peak wear at 45°, followed by a decrease in wear down to the minimum wear rate at 90°. Significant differences were observed in the mass loss of the HCCI samples: the samples eroded at 45° showed a mass loss 2.7 times greater than the eroded condition at 90°, indicating that, due to the condition of slurry contact with the surface of the samples, erosive and abrasive mechanisms acted synergistically favoring wear at 45°. On the other hand, samples eroded at 30° and 60° showed similar and intermediate mass losses. In general, for the samples eroded at a normal angle (90°) the mechanisms of wear due to plastic deformation of the matrix and carbide fracture were observed, while for smaller angles, the mechanisms of micro cutting and micro grooving were more evident.

Keywords: Wet erosive wear; High chrome cast iron (HCCI); Slurry pumps; Impact angle variation

1. Introduction

Tribology encompasses studies focused on friction, wear and lubrication and, thus, is defined as the Science and Technology of the interaction between surfaces in relative motion and the particles inserted therein [1].

According to ASTM G40-17 wear is defined as the alteration of a solid surface due to the progressive loss of material due to the relative movement between the contact of that surface with other materials. Wear, in general, is considered the main cause of loss of material and mechanical performance in industrial equipment, directly compromising the reliability and useful life of such equipment. Wear rates show drastic changes depending on the operating conditions and the materials selected for the construction of the equipment, these being the two most important factors for wear control in the industry [2,3].

Erosive wear is represented by the progressive loss of material from a surface due to mechanical interaction when liquid or solid particles collide on a surface. In wet erosive wear, there is a process of collision and transfer of kinetic energy from an erosive slurry (solid particles mixed in liquid) to a surface, generating high local contact stresses and promoting

* Corresponding author: Rodrigues da Costa Adilson

Copyright © 2023 Author(s) retain the copyright of this article. This article is published under the terms of the Creative Commons Attribution Liscense 4.0.

the removal of material from that surface. Erosion depends mainly on the surface properties of the eroded material, the solid particle properties, the slurry flow characteristics and the geometric conditions of the impact [4,5,6].

During the transport of slurries, wear modes by abrasion, corrosion and erosion may occur. Among these, erosion is responsible for most wear and material removal from components subject to wear processes. Erosion and abrasion present some similarities, however in erosion the transfer of kinetic energy from the particle to the wear surface occurs, while in abrasion the loss of material is due to the displacement of hard particles subjected to the action of compressive force [4].

Wet erosive wear usually occurs under conditions of turbulent flow at the time the slurry hits a surface causing material removal, and is often observed in slurry pump rotors and pipelines for ores transportation [4,7].

Slurry pumps are flow machines or turbo-machines used to transfer abrasive slurries by converting rotational kinetic energy into hydrodynamic energy for the fluid. This equipment is widely used for the hydraulic transport of solids (mud, clay, sludge, sand, ores and tailings in the solid size range of up to 2 mm) over short, medium or long distances through ducts (pipes) [8].

The service life of a slurry pump can range from weeks to a few years depending on the type of abrasive slurry conveyed. Direct costs related to wear on these equipment components are significant for the mining industry and reducing these costs requires a better understanding of pump wear patterns and wear rates caused by different slurries in different impeller geometries [9].

Among the main components of slurry pumps, the impellers are the ones that generally show the highest rates of wear during operation. Wear occurs mainly by erosion due to the impact of solid particles, but cavitation and corrosion processes can also be present [10,11].

In the specific case of slurry pump rotors, with the variation in the geometry of the blades along the rotor, there is a variation in the angle of attack of the erosive particles, ranging from shallow angles (wear mechanisms similar to abrasion at low tension) to high impact angles. Wear mechanisms related to high stress abrasion can also occur due to the crushing of abrasive particles trapped between the rotor blades and the volute [12].

There are several materials used to manufacture the components of slurry pumps: from the numerous cast irons with high wear resistance, passing through high resistance steels (FeCrC alloys), rubbers and elastomers. The most used are abrasion resistant white high chromium cast irons (ASTM A532).

High chromium cast irons are ferrous alloys containing 11–30% by mass of Cr and 1.8–3.6% by mass of C, and may also contain alloying elements such as molybdenum, manganese, copper, nickel, niobium, among others. This material can be considered as a composite material because it is formed by a metal matrix reinforced with hard carbide particles and is generally used in components that operate under extreme wear conditions, such as, for example, slurry pumping systems in mineral industry processes, coal, cement, ... [13,14].

The excellent resistance to wear and corrosion of high-chromium cast irons is strongly related to their microstructure, which usually presents a hard second phase composed of primary carbides or M_7C_3 eutectics of high hardness present in a martensitic, austenitic matrix or a product of the transformation of these microconstituents. The high hardness of the carbides provides good resistance to abrasion, while the toughness of the matrix provides good resistance to impacts during the wear process [15].

In order to evaluate the impact angle effect on the erosive wear resistance of a high chromium cast iron, wet erosive wear tests were carried out by varying the slurry impact angle on samples from a slurry pump impeller. For this purpose, suitable equipment was developed.

2. Material and methods

The high chromium white cast iron (HCCI)) specimens were obtained by cutting the cross-section of the blade region of a slurry pump rotor for transporting iron ore in the dimensions of 25x25x0.5mm by wire erosion.

The material has the typical composition of a hypereutectic high chromium cast iron with a content of 27%Cr and other alloying elements such as nickel, molybdenum and niobium (Table 1). Table 2 shows the HRC and HV_{30} hardness of the material.

Table 1 Chemical composition of high chromium cast iron

Element (%wt)	Cr	Ni	Mo	Nb	Fe
	27	0.183	0.18	0.024	Balance

Table 2 HRC and HV_{30} hardness of high chromium cast iron samples submitted to erosive and abrasive wear tests

High Chromium Cast Iron		
	Hardness	**St. dev.**
HRC	58.9	0.62
HV30	708	17.05

In order to observe the microstructure of the HCCI, the metallographic preparation of the samples and chemical attack with Vilela reagent were performed**.**

Optical micrographs of the material are shown in Figure 1. The presence of primary carbides with two distinct morphologies was observed: elongated primary carbides and polygonal primary carbides with hexagonal morphology, in addition to the presence of M_7C_3 eutectic carbides in a martensitic matrix. The material presented about 35%±2.34 of volumetric fraction of carbides calculated through image analysis using the Olympus Stream Essentials software.

Vickers microhardness analysis indicated that the carbides had an average hardness of 1557±77 $HV_{0.05}$ while the matrix had 700±9.6 $HV_{0.30}$.

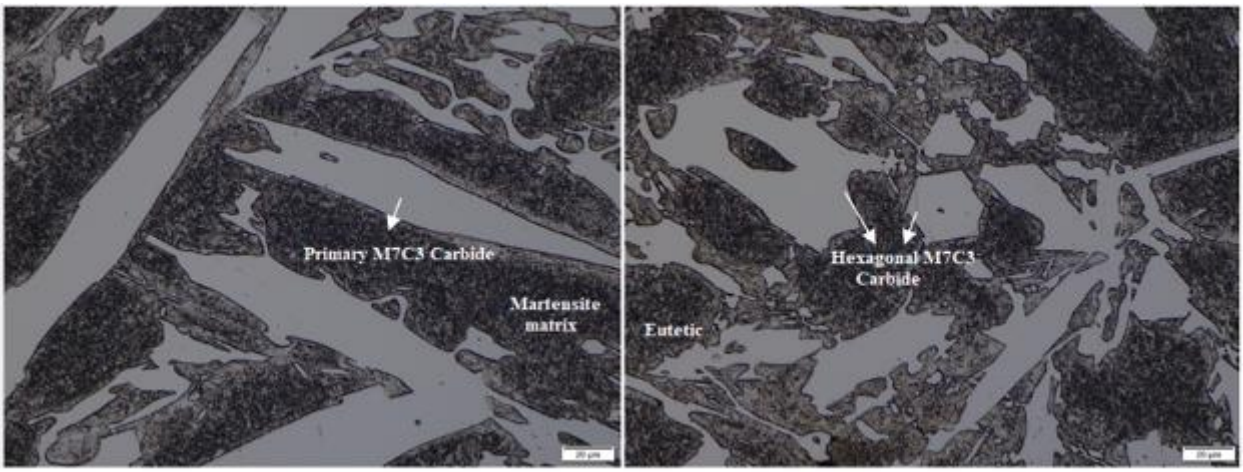

Figure 1 Optical micrography of high chromium cast iron. 500x magnification

To evaluate the variation of the impact angle of the slurry on the HCCI, wet jet erosive wear tests were carried out, varying the angle of incidence of the slurry in 30°, 45°, 60° and 90° and the distance of 25mm between the end of the injector tube and sample holder. IPT n100 standard silica sand was used as abrasive forming a slurry with a concentration of 20% by weight. The test time was set at 12 minutes with cleaning and weighing of samples every 2 minutes.

The samples were impacted with an average flow of 3g/s of silica sand, totaling approximately 2.16kg of abrasives during the 12 minutes of testing.

3. Results

3.1. Development of the wet erosion equipment

The wet erosive wear test was planned for the experimental determination of the mass loss caused by the interaction of an abrasive slurry projected on samples of interest at different angles.

The equipment developed, as can be seen in Figure 2, consists of a main reservoir of solid particles (abrasives) (RA) and a secondary reservoir containing water (RH). Both reservoirs are pressurized by an air compressor and the water/abrasive mixture (slurry) is projected through an injector tube (TI) onto the sample of interest (PA). Figure 2 shows overall details of the equipment's components and the injector and sample holder.

The erosive wear is evaluated from the loss of mass of the sample in relation to the test time, being possible to vary the concentration of the slurry, the type of abrasive, the impact angle and the distance from the tip of the injector to the sample holder.

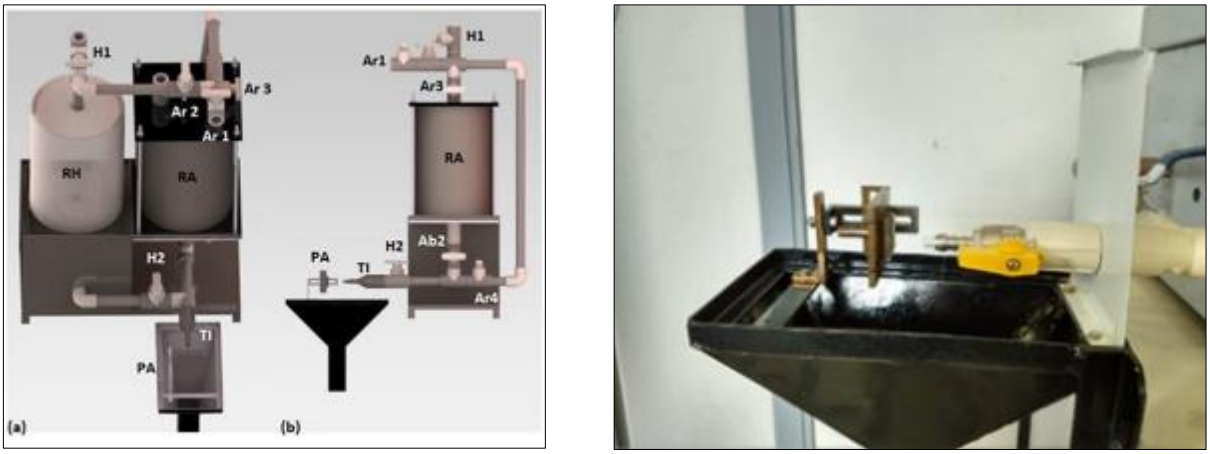

a, b c

Figure 2(a, b, c) Equipment for wet erosion testing. Front view (a). Side view (b). (c) Injector and sample holder. Captions: RA- Abrasive Reservoir; RH- Water Reservoir; TI- Injector tube; PA- Sample holder; H1- Water supply valve; H2- Water flow valve for the main pressure piping; Ab1- Abrasive supply valve; Ar1- Compressed air supply valve connected to the compressor; Ar2- Water reservoir pressurization valve; Ar3- Abrasive tank pressurization valve; Ar4- Air flow valve towards the injector tube

The operational specifications of the equipment are shown in Table 3.

Table 3 Wet erosive wear equipment operating specifications

Equipment for wet jet erosive wear tests.				
Parameter	**Min**	**Max**	**Unit**	**Characteristic**
Injector diameter		4,5	mm	Constant
Sample holder angle	15, 30, 45, 60, 75, 90		º	Variable
Sample-Injector distance	20	50	mm	Variable
Slurry concentration	15	40	[%Vol]	Variable
Water Flow	0,9		l/min	Constant
Abrasive Flow	237		g/min	Variable
Abrasive Reservoir	10		kg	Content
Water Reservoir	5		L	Content
Sample Size	25 x 25 x 0,5		mm	Variable

3.2. Erosive wear test with impact angle variation

The macroscopic wear surfaces of the samples eroded at angles of 30°, 45°, 60° and 90° are shown in Figures 3. In Figure 4 the mass loss and wear rates obtained after the tests and in Figure 5 the wear mechanisms related to the different impact angles.

The difference between the topographies of wear surfaces formed after erosive wear is evident. The samples tested at 90º presented the wear surface in the shape of a well-defined circular cap, while the samples tested at smaller angles presented surfaces in the shape of elongated ellipses due to the contact condition of the erosive particles with the surface of the samples.

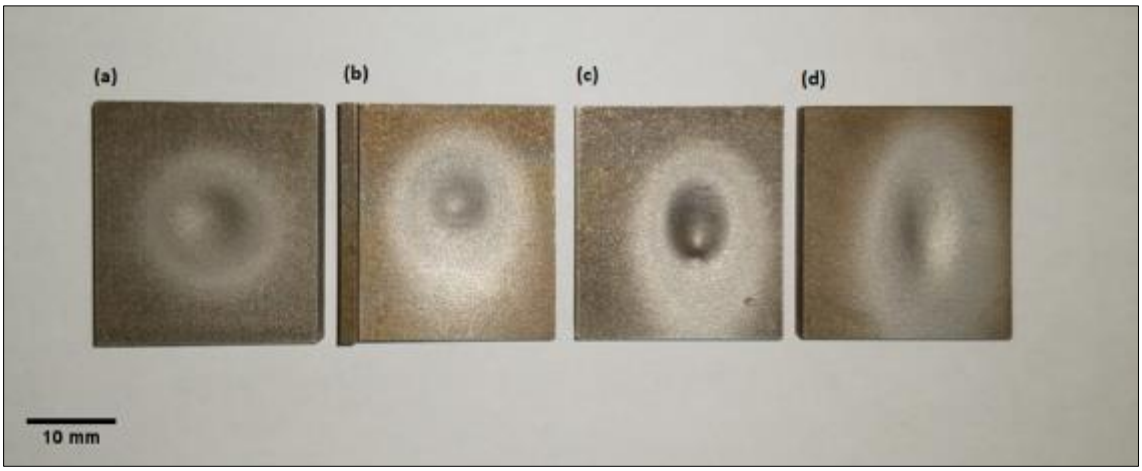

Figure 3 Erosive wear test. Macroscopic wear surface of the tested samples. (a) 90°; (b) 60°, (c) 45° and (d) 30°

It is observed that the peak of erosive wear occurred at the angle of 45° with a subsequent decrease in wear at larger angles. According to Figure 6, the samples worn at a normal angle showed the lowest mass loss (97mg), followed by the samples tested at 60° (142mg) and 30° (162mg), while, for the samples at 45°, the mass loss reached values of 274mg. The erosive wear at 45° was then 2.8 times greater than the erosive wear at 90°, 1.9 times greater than that at 60° and 1.7 times greater than that at 30°.

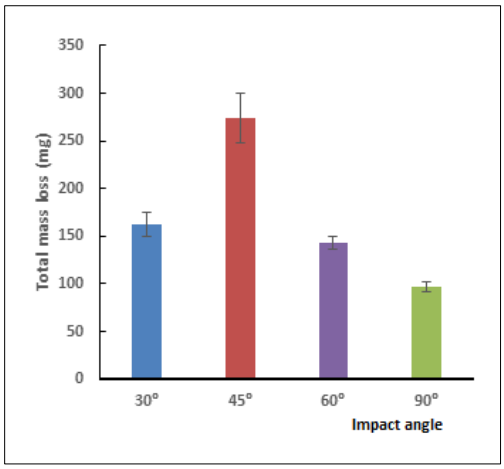

Figure 4 Wet erosive wear test. Total mass loss in relation to the test time and impact angle. Samples tested at angles of 30°, 45°, 60° and 90° during 12 minutes

Erosion has the typical characteristic of variation in wear rate in relation to the variation in impact angle. Generally, the wear rate is maximum at shallow angles for ductile materials and this angle tends to increase the lower the ductility of the material until reaching values close to 90° for brittle materials.

The erosive wear rate was calculated from the ratio between the mass loss of the samples in relation to the mass of abrasive that impacted the wear surface. The tests took place with an average flow rate of 0.9 l/min of water to form a

slurry with 10% by volume of IPT n100 standard sand. For this, the samples were impacted with an average flow of 3g/s of silica sand, totaling 2.16kg of abrasive during 12 minutes of testing.

From the results, Figure 7, it is possible to observe a typical pattern of the wear rate in relation to the angle variation during erosive wear [16,17]. First, at smaller angles, there is an increase in mass loss until the wear peak is reached at a specific angle, and then there is a decrease in wear with increasing impact angle up to 90°.

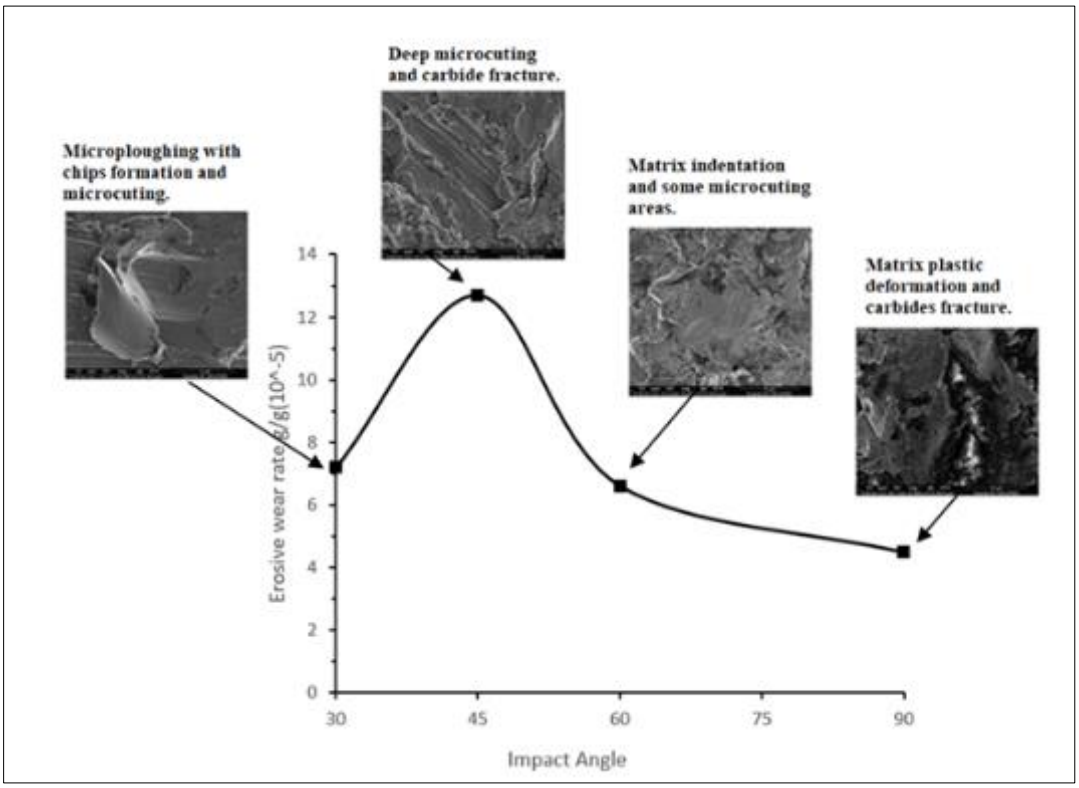

Figure 5 Variation of wear mechanisms and erosion rate with impact angle for HCCI samples

The curves of accumulated mass loss in relation to the test time for each condition of impact angle are represented in Figure 6. The behavior in permanent regime of wear can be observed by the linear adjustment curves applied to the accumulated mass loss after the total test time. All curves could be fitted with a first-degree straight line (y=ax+b) obtaining R^2 very close to 1. It was not possible to observe the run-in process from weighing the samples every 2 minutes of the test.

Samples eroded at angles of 30° and 60° showed similar mass loss curves throughout the test with intermediate mass losses to those of samples eroded at 45° and 90°. In the first 2 minutes of the test, the wear of the samples eroded at 30°, 45° and 60° approached, but from then it is possible to observe the greater severity of the jet projected at 45°. The samples eroded at 90° presented the lowest mass losses throughout the test.

The variation in the wear rate of high chromium cast iron with the variation in the impact angle of the slurry is of great importance for the tribological study of the internal components of the slurry pumps, as the abrasive particles impact the internal components at different angles during the pumping of a slurry between the suction point, the contact with the rotor blades and the pump discharge point. As observed in the experiments, the resistance to erosive wear of high chromium cast iron varies in relation to the angle of impact of the abrasive particles, observing the different predominant wear mechanisms. This information must, above all, be taken into account when designing a slurry pump to avoid premature failures resulting from regions where certain particles impact angles would cause more severe wear.

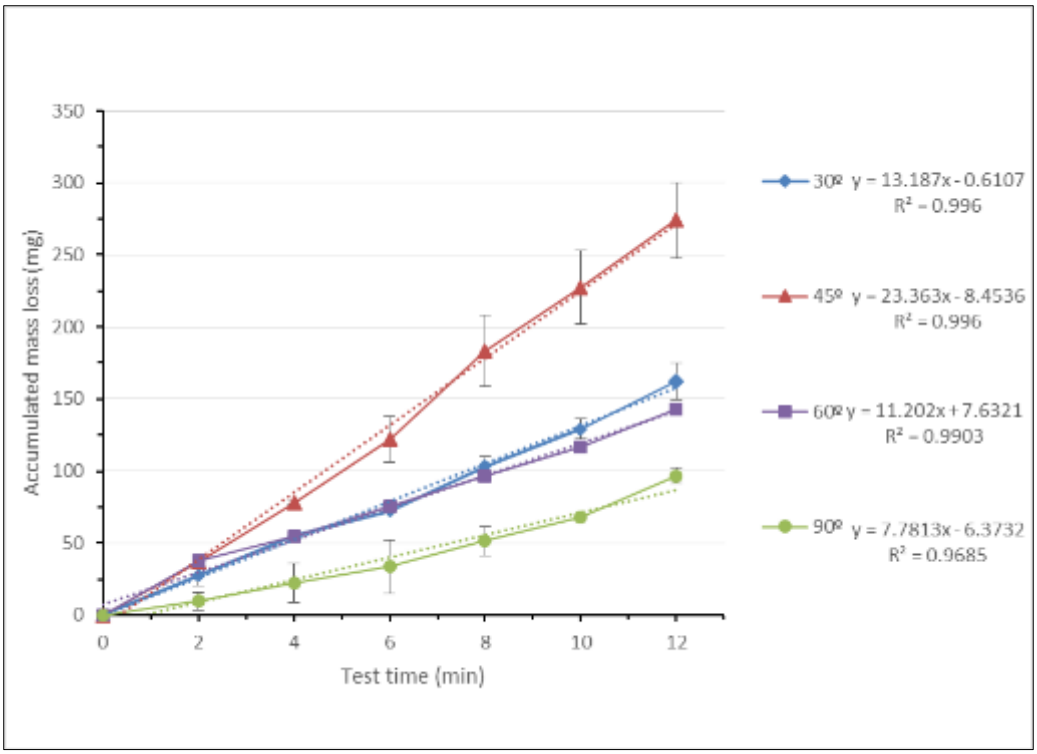

Figure 6 Wet erosive wear test. Accumulated mass loss in relation to the test time of high chromium cast iron samples at angles of 30°, 45°, 60° and 90°

4. Discussion

Wet erosive wear (slurry) differs from dry erosive wear considering the medium in which solid particles are dispersed. The viscosity of water is about 100 times greater than the viscosity of air and some gases, thus causing a greater influence on solid particles behavior during impact with the wear surface. When a jet of fluid impacts on a flat surface, the spreading of the fluid along the surface occurs. In wet erosion, the solid particles tend to follow the movement of the slurry flow due to the higher viscosity of the liquid and thus the actual angle of impact of the solid particles tends to be different from the nominal angle of the slurry jet [16].

In Figure 7, the effect of spreading a slurry jet over a flat surface is represented, where V represents the nominal direction of the slurry jet and V1 and V2 the directions after the impact and spreading of the slurry. The actual impact angle of abrasives moving in the V1 direction is smaller than the nominal jet angle while abrasives in the V2 direction impact at greater angles. As most abrasives move in the V1 direction, for angles smaller than 90°, it can be considered that the actual impact angles of the particles will be smaller than the nominal angle of the slurry jet. The amount of abrasives following the V1 direction will be greater the smaller the nominal angle of the slurry jet. Thus, smaller impact angles will have greater amounts of abrasive sliding over the sample and elongating the worn surface. With the increase of the impact angle, the amount of abrasives in the V1 direction decreases and there is an increase in V2, also increasing the impact component of the particles, until reaching the angle of 90°, in which the two scattering directions V1 and V2 tend to be equal with the maximum impact component, thus forming a worn surface in the form of a circular cap. This spreading effect of the slurry jet can be observed on the worn surfaces of the eroded samples (Figure 3) where the surface becomes less elongated with the increase of the impact angle indicating that the sliding component caused by the abrasives decreases with the same increase of the angle.

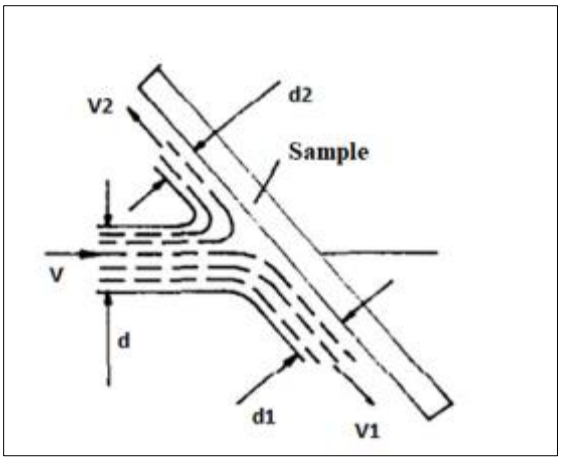

Figure 7 Effect of spreading the slurry jet over a flat surface. (FUYAN & HESHENG, 1991)

The tangential and surface normal components from the velocity of solid particles are responsible for material displacement and surface indentations, respectively. As the impact angle increases, the normal component increases and surface material is generally removed due to particle indentations and plastic deformations. As the impact angle decreases, the normal component tends to become smaller, increasing the tangential component to the surface, thus favoring the formation of increasingly elongated craters and the mechanisms of micro cutting and grooving [17].

This behavior can be observed on the surfaces tested at different angles on the high chromium cast iron samples.

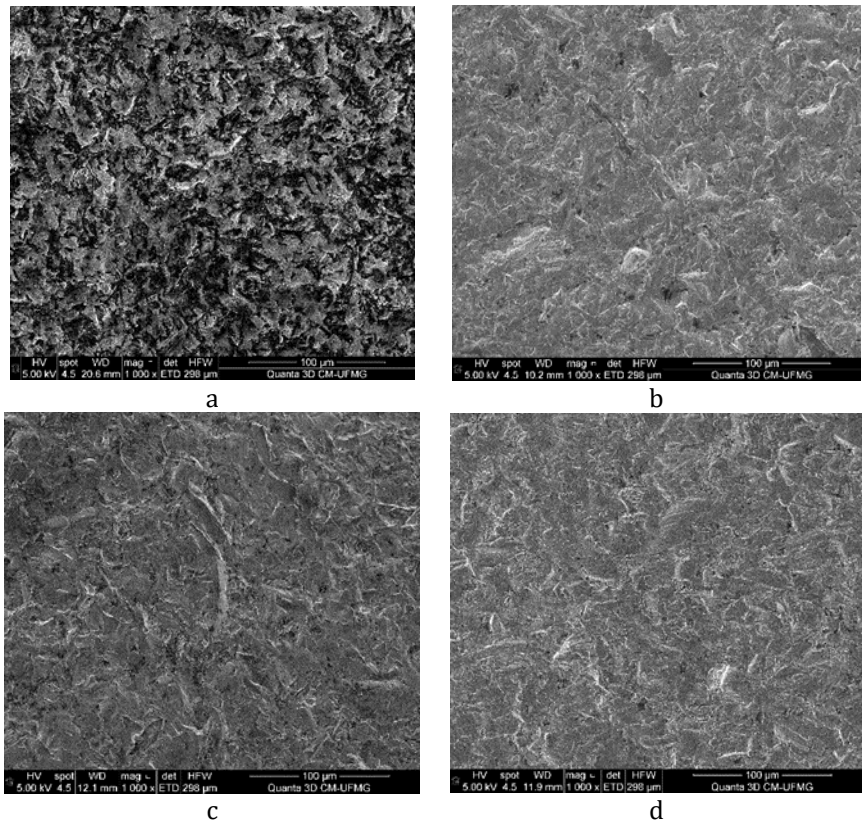

Figure 8 SEM images of the worn surface of the eroded samples: (a) 90°. (b) 60°. (c) 45°. (d) 30°

It is possible to observe, in samples eroded at 30° and 45°, the direction of the erodent flow over the surface. Due to the impact angle, wear tracks were formed due to the sliding of abrasive particles over the surface in the flow direction. In the samples eroded at 60°, characteristic regions of indentation of the particles on the surface are observed, while some wear tracks due to the sliding of particles can also be observed. This behavior is due to the larger normal component of impact in relation to the tangential component at this angle. For samples eroded at 90°, in general, a typical surface of

particle indentations is observed not showing a directional characteristic, but, at higher magnifications, occasionally, wear tracks are observed in discrete regions, probably attributed to changes on the movement of particles at the moment of impact, either by deviation caused by the local turbulence of the slurry flow itself or by the deviation of the collision of rebound particles.

The erosion condition at a normal angle of the high chromium cast iron samples resulted in less mass loss when compared to the conditions at smaller angles. At a 90° angle, the erosion mechanisms are related to material embrittlement usually due to the repeated impact of hard particles causing the formation and propagation of cracks. The progression of this mechanism results in surface fatigue and material tearing.

Observing the trajectory of these particles, it can be inferred that there is an interference effect between possible collisions of the particles that impact the wear surface and return in the opposite direction with the particles that are leaving the injector tube on the way to the sample. These collisions can cause the underlying particles to slow down or change their trajectory. Evidence of deviations from the designed trajectory of the particles can be observed by the color change of the worn surface (Figure 3). The interference of rebound particles may have contributed to the decrease in the kinetic energy of the deviated particles as well as the decrease in the number of particles that effectively impacted the wear surface.

Craters formed by the penetration of abrasive particles into the martensitic matrix in the normal angle impact condition are observed. Some of these particles remained embedded in the surface after wear (Figure 9), mainly at angles of 90° and 60°. For the other angles, abrasive incrustation was not observed.

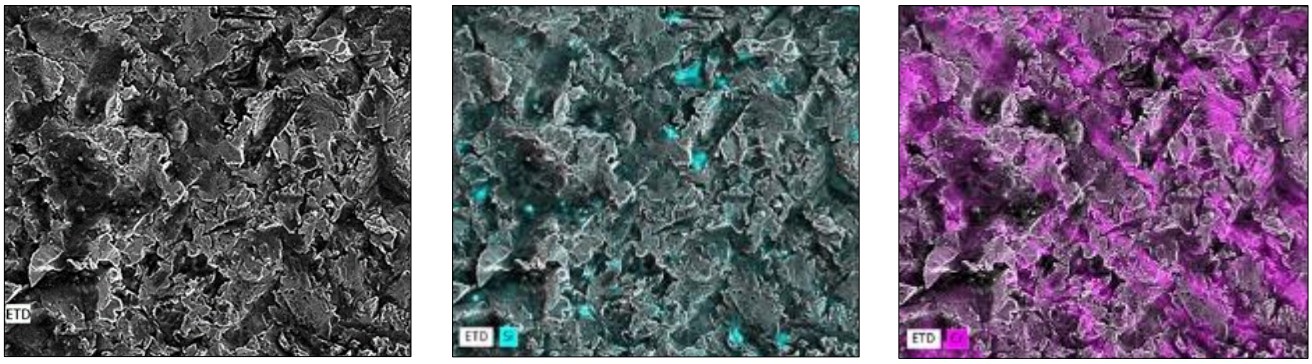

a b c

Figure 9 SEM/EDS. (a) Wear surface at 90°. (b) Si chemical composition map. (c) Cr chemical composition map

The surface of a material plastically deforms once the yield strength is exceeded. For an erosive particle to be able to plastically indent a surface, the hardness of this particle (Ha) must be at least 1.2 times greater than the hardness of the surface (Hs), i.e., Ha/Hs>1.2 [19].

The hardness of martensitic matrix of the HCCI is approximately 700Hv and the carbides around 1560Hv while the silica, according to the literature, presents an average hardness between 800 and 1200Hv. Given this, it is reasonable to infer that the relationship between the minimum hardness for particle indentation (Ha/Hs>1.2) was achieved for the martensitic matrix.

The greater loss of mass at the angle of 45° can be interpreted considering the normal and the tangential components acting together: plastic deformation by sliding of the particles being responsible by cutting and grooving mechanisms associated with impact indentations. Thus, the synergistic effects of erosive and abrasive wear modes act in the same tribosystem promoting more efficient material removal [18].

Figure 10(c) shows the worn surface at 30°. Large regions of matrix micro-cutting, fracture and carbide pulling are observed. The wear of the matrix (martensite), from cutting and grooving mechanisms, left the carbides exposed and these could be pulled out due to the progress of wear. There is also a greater directionality of the deep scratches generated by the micro cuts towards the drag generated by the flow of the slurry and large regions of grooving with the formation of chips and lateral displacement of material. Both chips and displaced materials are pulled out as wear progresses.

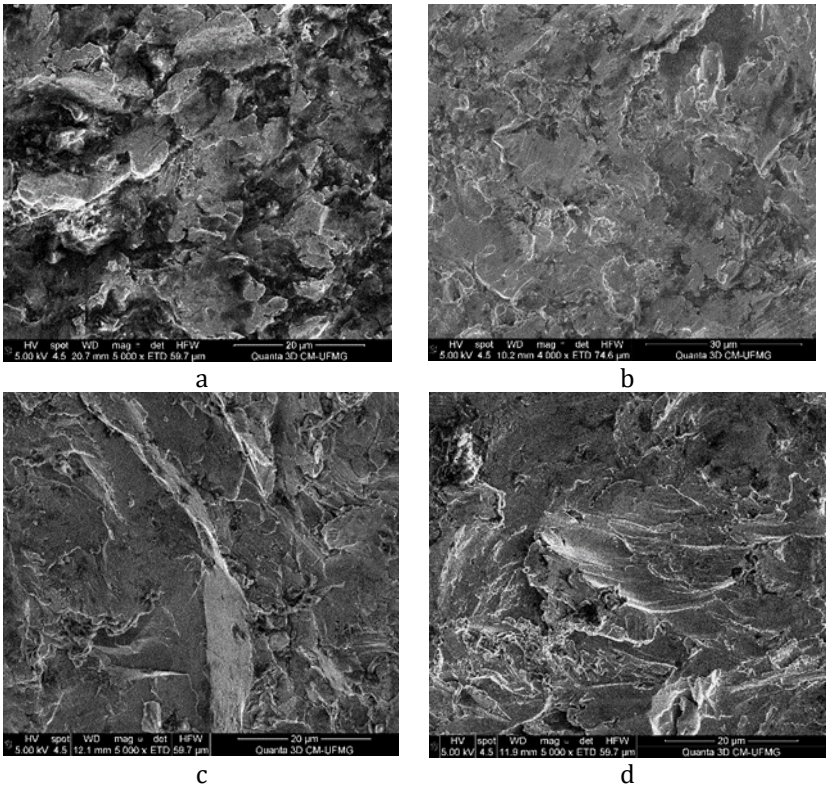

Figure 10 SEM images of the wear surface of the eroded samples: (a) 90°. (b) 60°. (c) 45°. (d) 30°

In the region of greater depth of the worn surface, it is expected to find erosive and abrasive micro mechanisms acting together, increasing the severity of the wear. It can be seen that, in Figure 6, the samples tested at 30° and 45° showed similar mass losses in the first 4 minutes of the test, but in the subsequent minutes there was an expressive greater mass loss of the samples at 45°, showing that this region also behaved as a wear concentrator region, with the progression of wear, becoming a conditioning region for the flow of the erosive slurry jet.

For the angle 30º, an elongation of the crater is observed compared to the larger angles and the formation of a surface in the shape of a large groove (Figure 5). In this condition, there is also the interaction of abrasive wear mechanisms together with erosive wear mechanisms, but due to the elongated shape of the crater it is likely that there was a dominance of abrasive mechanisms, (micro cutting, scratching and micro grooving), with probable longer interaction times of the erosive particles in contact with the sample compared to the 90° angle. At smaller angles, there is a greater probability that the erosive particles remain in contact with the worn region for a longer time, as there is a greater tendency for the particle to remain in contact with the surface due to its deflection after contact, favoring micro mechanisms of abrasion.

The images of the eroded surface at 30° show very clear the shallow drag mode of the ductile material (matrix). From the visualization of Figures 8(d); 10 (d) and 11, it is indicated that there was a prevalence of cutting and grooving, which are mechanisms of sliding abrasion.

Under 45° angle, the normal component (impact) is higher than at 30°, while the opposite occurs for the tangential (abrasive) component of wear. The smaller loss of mass of the material under wear at 30°, when compared to the angle of 45°, can be explained due to the action of the hard carbides on the surface of the material, resisting the dominance of abrasive wear mechanism at this angle.

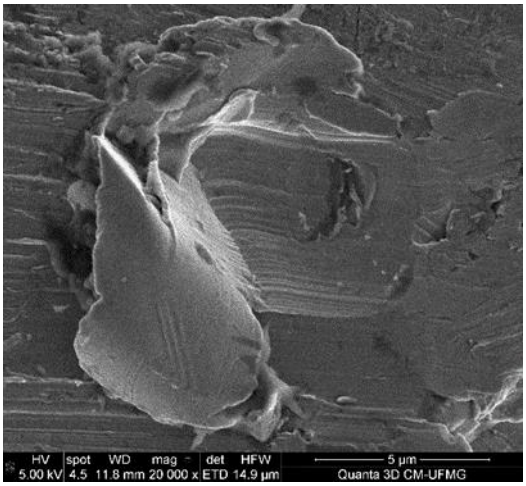

Figure 11 Worn surface at 30°. Micro cutting mechanism with the formation of adjacent ridges and frontal bow

Samples tested at 60° and 30° achieved very similar wear rates over the course of the tests. For the 60° angle, unlike the 30° angle, the normal component tends to be greater than the tangential component: generally, the indentations of solid particles on the surface prevail over abrasive mechanisms (Figure 10(b)). The worn surface appears less elongated than the 45° and 30° surfaces, as expected due to the dynamics of contact and spreading of the slurry flow with the surface. As already reported in the literature, the angle of 60° represents a flow geometry with which the decrease in the wear rate show similarities with the wear rates angles close to 30°.

5. Conclusion

The equipment for evaluating wet jet erosive wear developed in this project showed satisfactory results and good reproducibility. It presents a good alternative for the evaluation of materials subject to wet erosive wear based on the variation of the impact angle of the slurry, and can also carry out tests varying the composition, concentration and pH of the mixture allowing evaluate the synergy between erosion-corrosion.

The results of the tests demonstrated that the wet erosive wear of the high chromium cast iron (27%Cr) with martensitic matrix analyzed in this work follows a classic pattern of variation of the erosive wear rate with the increase of the slurry impact angle. There is an increase in the wear rate with increasing angle until reaching the highest wear peak at 45° followed by a continuous decrease until the lowest wear angle (90°).

Wet erosive wear at different angles caused significant differences in the mass loss of the HCCI samples. The samples eroded at 45° showed a mass loss 2.7 times greater than the condition with less wear at 90°. Samples eroded at 30° and 60° showed similar mass losses throughout the erosion test and intermediate ones at angles of 45° and 90°.

The worn surfaces observed showed distinct topographies starting from a circular cap at a 90° angle followed by more elongated craters the smaller the erodent impact angle. This topographical variation is explained by the dynamics of erodent contact and the effect of flow scattering on the sample surface.

At the angle of 30°, the tangential component is greater than the impact component, favoring the action of abrasion mechanisms. At 45°, the peak of wear severity occurred indicating that erosive and abrasive mechanisms may have acted synergistically. As the angles increase, there was an increase in the impact component up to the 90° angle, when the erosion mechanisms attain lower rates.

In general, mechanisms due to plastic deformation of the matrix and carbide fracture are present in samples eroded at normal angle while micro cutting and micro grooving prevail for smaller angles.

Compliance with ethical standards

Acknowledgments

EM/UFOP – Ouro Preto School of Mines/Federal University of Ouro Preto.

REDEMAT- Thematic Network in Materials Engineering.

ITV- Mineração. Vale Technological Institute – Mining.

Disclosure of conflict of interest

The authors declares that there are no conflicts of interest in connection with this paper.

References

[1] Halling J. (Ed.). (1975). Principles of tribology. London Macmillan. ISBN 0333154967. 401 p.

[2] Bhushan B. Tribology of Earthmoving, Mining, and Minerals Processing. In: Modern Tribology Handbook, Two Volume Set. CRC Press. (2000) 1361-1400. https://doi.org/10.1201/9780849377877.

[3] Stachowiak G, Batchelor AW. (2013). Engineering tribology. Butterworth-Heinemann. 884 p.

[4] Javaheri V, Porter D, Kuokkala Veli-Tapani. (2018). Slurry erosion of steel–Review of tests, mechanisms and materials. Wear, 408-409, 248-273. https://doi.org/10.1016/j.wear.2018.05.010

[5] Costa AR. Tribology applied to mining: concepts and applications. (2021) First edition (in Portuguese). Fontenele Publications. Sao Paulo, Brazil.

[6] ASTM International. (2017). ASTM G40-17 Standard Terminology Relating to Wear and Erosion. West Conshohocken, PA; ASTM International.

[7] Chandel S, Singh SN, Seshadri V. (2012). Experimental study of erosion wear in a centrifugal slurry pump using coriolis wear test rig. Particulate Science and Technology, 30(2) 179-195. https://doi.org/10.1080/02726351.2010.523926

[8] Tarodiya R, Gandhi BK. (2017). Hydraulic performance and erosive wear of centrifugal slurry pumps-A review. Elsevier. Powder Technology, 305, 27-38.

[9] Walker CI. (2001) Slurry pump side-liner wear: comparison of some laboratory and field results. Wear, 250(1) 81-87. DOI: 10.1016/S0043-1648(01)00613-5

[10] Khalid YA; Sapuan SM. (2007). Wear analysis of centrifugal slurry pump impellers. Industrial Lubrication and Tribology. ISSN: 0036-8792

[11] Perez RX, Conkey AP. (2016). Troubleshooting Rotating Machinery: Including Centrifugal Pumps and Compressors, Reciprocating Pumps and Compressors, Fans, Steam Turbines, Electric Motors, and More. Scrivener Publishing LLC.
Co-published by John Wiley & Sons, Inc. Hoboken, New Jersey, and Scrivener Publishing LLC. Salem, Massachusetts. ISBN 978-1-119-29413-9

[12] Llewellyn RJ, Yick SK, Dolman KF. (2004). Scouring erosion resistance of metallic materials used in slurry pump service. Wear, 256(6) 592-599. https://doi.org/10.1016/j.wear.2003.10.002

[13] Shaoping Z, Shen Y, Zhang H, Chen D. (2015). Heat treatment effect on microstructure, hardness and wear resistance of Cr26 white cast iron. Chinese Journal of Mechanical Engineering, 28; 140-147.

[14] Chen, Ling et al. (2015). Characterization of microstructure and mechanical properties of high chromium cast irons using SEM and nanoindentation. Journal of Materials Engineering and Performance, 24(1) 98-105. DOI:10.1007/s11665-014-1245-8

[15] Adler TA, Doğan ÖN. (1999). Erosive wear and impact damage of high-chromium white cast irons. Elsevier. Wear, 225, 174-180. Parte superior do formulário Parte inferior do formulário

[16] Fuyan L, Hesheng S. (1991). The effect of impingement angle on slurry erosion. Wear, 141; 279-289.

[17] Nandre BD, Desale GR. (2018). Study the Effect of impact angle on slurry erosion wear of four different ductile materials. Materials Today: Proceedings, 5(2) 7561-7570. DOI 10.1016/j.matpr.2017.11.428

[18] Gates JD. (1998). Two-body and three-body abrasion: a critical discussion. Wear, 214, 139-146.

[19] Hutchings I; Shipway P. (2017). Tribology: Friction and Wear of Engineering Materials. Butterworth-Heinemann. ISBN-10: :13-ISBN 0081009100 0081009109-978